



ELSEVIER

Carbohydrate Research 304 (1997) 191–208

CARBOHYDRATE  
RESEARCH

# Structural analysis of the lipopolysaccharide from *Vibrio cholerae* serotype O22

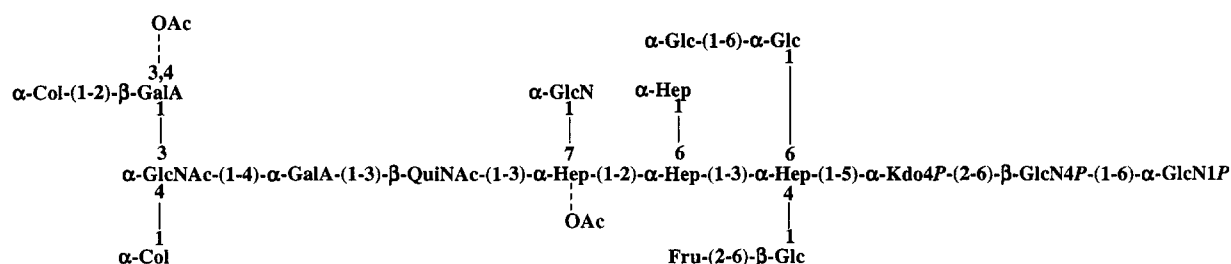
Andrew D. Cox<sup>\*</sup>, Jean-Robert Brisson, Pierre Thibault,  
Malcolm B. Perry

*Institute for Biological Sciences, National Research Council, Ottawa, ON, Canada K1A 0R6*

Received 12 May 1997; accepted 7 July 1997

## Abstract

The structure of the lipopolysaccharide (LPS) from *Vibrio cholerae* serogroup O22 was elucidated. The LPS was subjected to a variety of degradative procedures, and the structures of the purified products were established by monosaccharide and methylation analyses, nuclear magnetic resonance (NMR) spectroscopy, and mass spectrometry. The following structure for the complete LPS molecule was determined on the basis of the combined data from these experiments.



The elucidation of this structure provided a chemical basis for the serological cross-reactions observed between this strain and *V. cholerae* serogroup O139. © 1997 Elsevier Science Ltd. All rights reserved

**Keywords:** *Vibrio cholerae* O22; LPS; NMR; Mass spectrometry

<sup>\*</sup> Corresponding author. Institute for Biological Sciences, 100, Sussex Drive, National Research Council, Ottawa, ON K1A 0R6 Canada. Tel.: +1-613-9911674; fax: +1-613-9529092; e-mail: andrew.cox@nrc.ca.

## 1. Introduction

*Vibrio cholerae* serotype O139 first gained prominence in 1993 [1], as it was shown to be only the second strain of *V. cholerae* (serotype O1 strain being the first) capable of causing a cholera epidemic. It was subsequently revealed that serotype O139 originated from the serotype O1 strain by virtue of a rearrangement in the lipopolysaccharide (LPS) biosynthesis genes, whereby the DNA cluster responsible for O-antigen biosynthesis of serotype O1 was removed, whilst ca. 35 kb of new DNA, which encodes serotype O139 surface polysaccharide was acquired [2–4]. As expected, structural analysis of the O139 strain revealed an altered structure from the perosamine homopolymer of serotype O1, with serotype O139 possessing a complex O-antigen unit as illustrated in Fig. 1 [5,6]. Interestingly the O-antigen of serotype O139 consisted of only one O-antigenic unit; however, serotype O139 also produces a capsular polysaccharide of identical, polymeric O-antigen units [7,8].

*V. cholerae* serotype O139 was therefore essentially a camouflaged O1 strain, and this altered surface polysaccharide epitope enabled serotype O139 to avoid previously acquired host immunity to the serotype O1 strain, and this contributed significantly to the early success of the organism in producing epidemic cholera.

Several research groups have attempted to identify the bacterial strain that provided the DNA cluster responsible for the altered O-antigen structure. Initially, genetic studies identified *V. cholerae* serotypes O69 and O141 as possible donor strains [9,10]. However, a serological approach showed that the O69 and O141 antigens were not immunologically related to O139, but did identify two *V. cholerae* strains serotypes O22 and O155 that shared common epitopes with serotype O139 as well as possessing other

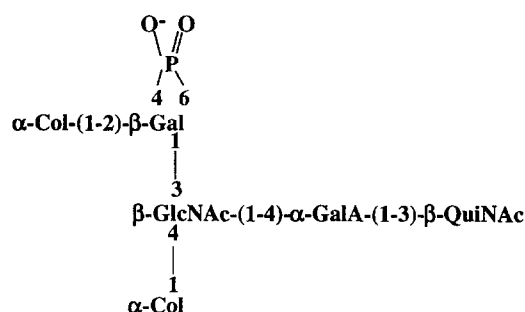


Fig. 1. Chemical structure of the O-antigenic repeat unit of the LPS of *V. cholerae* O139.

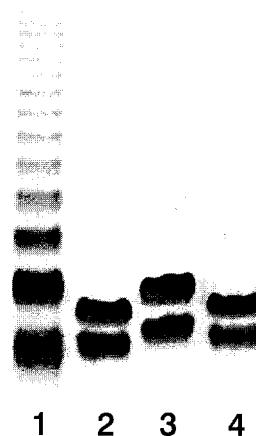


Fig. 2. DOC-PAGE pattern of LPS. (1) *Salmonella milwaukee* (S-type LPS; 5 µg); (2) *V. cholerae* O22 LPS (10 µg); (3) *V. cholerae* O139 LPS (5 µg); (4) *V. cholerae* O22 LPS (5 µg).

unique epitopes [11]. Subsequent compositional analysis of the O22 serotype revealed a very similar sugar composition to the serotype O139 strain [12]. In addition to the above evidence suggesting serotypes O22 and O155 as possible donor strains, a recent paper [13] analysing the sugar composition of all *V. cholerae* serotypes has supported this suggestion. Interestingly, serotype O22 was the only *V. cholerae* strain other than serotype O139 that produced the rare sugar, 3,6-dideoxy-L-xylo-hexose (colitose). A recent genetic study [14] has illustrated that DNA from serotypes O22, O141 and O155 is homologous to O139 DNA from the *rfb* region. Therefore, both genetic and serological data suggest serotype O22 as the possible donor strain.

This present study was, therefore, undertaken to elucidate the chemical structure of the LPS from *V. cholerae* serotype O22, which would enable a comparison to the structure of the serotype O139 strain. This structure may provide an explanation for the serological data and therefore add information to the consideration of O22 as a potential donor of the new genetic material in serotype O139.

## 2. Results

**Isolation and characterisation of the LPS.**—LPS from *V. cholerae* serotype O22 was isolated by the aqueous phenol method [15], yielding purified LPS (ca. 5%). No capsular material was isolated from this strain. DOC-PAGE analysis of the LPS (Fig. 2) showed that the characteristic 'ladder pattern' which

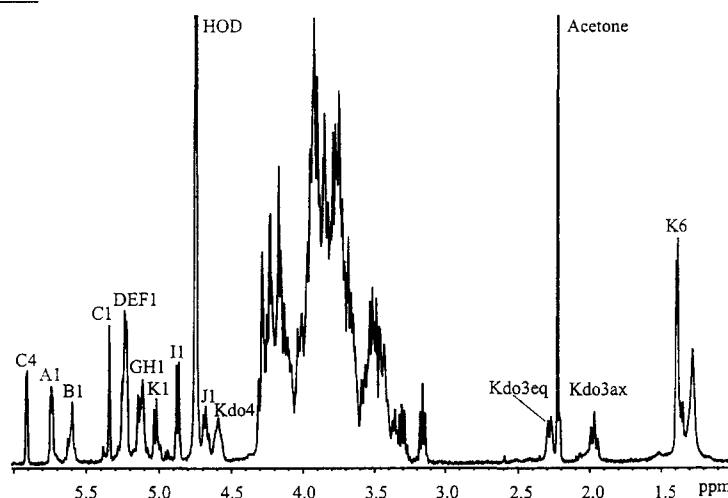
is indicative of a polymeric O-chain, was absent from this strain. As Fig. 2 shows, *V. cholerae* O22 LPS (lanes 2 and 4) migrates as two distinct bands, consistent with a lower band of unsubstituted core-lipid A and an upper band of core-lipid A with an additional homogeneous unit, possibly indicative of a mixture of R-type and SR-type LPS as was reported for *V. cholerae* O139 LPS (lane 3) [5].

**Compositional analysis.**—GLC–MS analysis of the derived alditol acetates and GLC analysis of acetylated (*S*)-2-butyl glycosides from the untreated LPS showed that it is composed of D-glucose (Glc), 2-amino-2-deoxy-D-glucose (GlcN), 2-amino-2,6-dideoxy-D-glucose (QuiN) and L-glycero-D-manno-

heptose (Hep). When the alditol acetates and acetylated (*S*)-2-butyl glycosides derived from mild hydrolysis of the untreated LPS were examined, 3,6-dideoxy-L-xylo-hexose (Col) and D-fructose (Fru) were identified. The presence of 2-amino-2,6-dideoxy-D-glucose and 3,6-dideoxy-L-glucose in the LPS, sugars both previously identified as constituents of the *V. cholerae* O139 O-antigenic repeat unit [6], are consistent with the previous compositional data [13] and the serological data suggesting that serotypes O22 and O139 may share a common epitope [11].

**Structural analysis.**—The KOH-treated LPS from *V. cholerae* O22 was initially examined in a  $^1\text{H}$  NMR experiment. The resulting spectrum was identi-

### b) O139



### a) O22

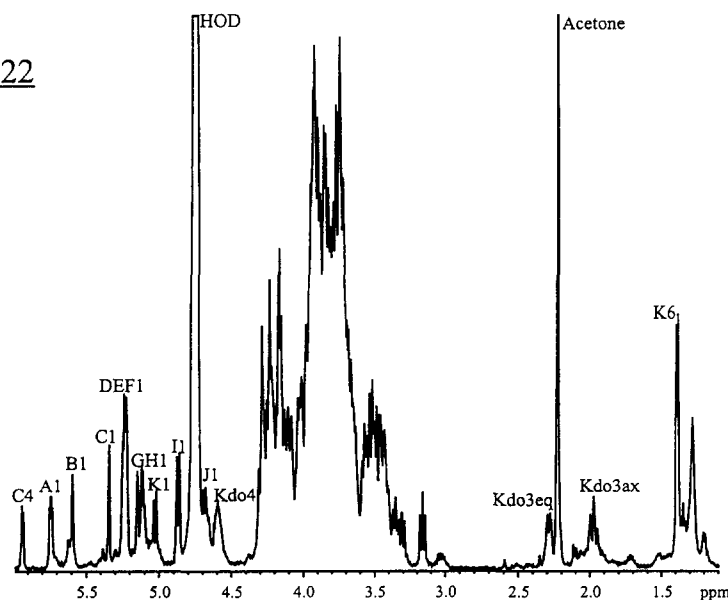


Fig. 3.  $^1\text{H}$  NMR spectra of the KOH-treated LPS from (a) *V. cholerae* O22 and (b) *V. cholerae* O139. The spectra were recorded in  $\text{D}_2\text{O}$  at pH 3.5 and 300 K.

cal to the spectrum obtained for *V. cholerae* O139 LPS following KOH treatment (Fig. 3). Further studies revealed that the COSY, TOCSY, NOESY,  $^{31}\text{P}$ – $^1\text{H}$  and  $^{13}\text{C}$ – $^1\text{H}$  HMQC spectra on the KOH-treated O22 LPS were all superimposable on those obtained for the O139 KOH-treated LPS sample [5].

These results show that the chemical structures of the two KOH-treated samples are identical, and it can be concluded that the  $\alpha$ -GalA-(1  $\rightarrow$  3)- $\beta$ -QuiN disaccharide of the repeating unit of serotype O139 is also present in serotype O22, thus providing a common epitope that may explain the serological cross reactions. However, the serological studies also suggested the presence of unique epitopes in the two strains, and, therefore, the remaining residues of *V. cholerae* O22 O-antigenic repeat unit need to be resolved.

To this end other degradative procedures were utilised. The deacylated, dephosphorylated, reduced-LPS [backbone-oligosaccharide (OS)] was fractionated on a Bio-Gel P2 column, and the resulting two fractions were initially examined by  $^1\text{H}$  NMR spectroscopy. Both fractions gave excellent NMR spectra. Two of the resonances in the high-field region (1.0–

2.5 ppm) of the 1D  $^1\text{H}$  NMR spectra could be attributed to the equatorial and axial methylene protons of the Kdo residue. In fraction 1, the doublet-of-doublets pattern characteristic of the equatorial H-3 proton was at 2.106 ppm ( $J = 4.0, 10.5$  Hz), in fraction 2 at 2.100 ppm ( $J = 4.0, 10.5$  Hz). The triplet indicative of the axial proton was at 1.784 ppm ( $J = 11.6, 11.6$  Hz) in fraction 1 and at 1.773 ppm ( $J = 11.6, 11.6$  Hz) in fraction 2. The chemical shifts of the methylene proton resonances from the Kdo residue indicated that it was in the pyranose ring form and has the  $\alpha$ -D-configuration [16]. As expected a crosspeak with a  $^{13}\text{C}$  coordinate of 36.32 ppm for fraction 1 and 36.27 ppm for fraction 2 in the 2D  $^{13}\text{C}$ – $^1\text{H}$  HMQC experiment could be attributed to the methylene carbon from the Kdo residue. Also in the high-field region of fraction 1 were signals at 1.997 and 1.888 ppm, which were tentatively assigned to the methyl protons of the acetyl groups. These signals were assumed to be indicative of incomplete removal of the N-acetyl groups by strong hydrazinolysis.

A further signal in the high-field region was a doublet at 1.338 ppm that was only present in frac-

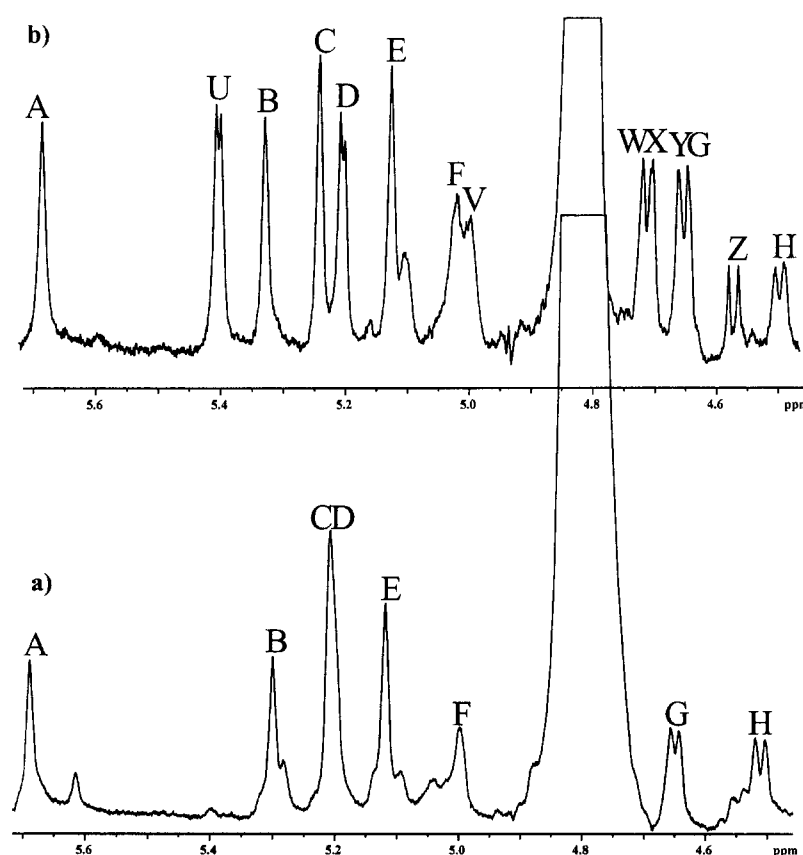


Fig. 4. Anomeric regions of the  $^1\text{H}$  NMR spectra of the backbone LOS (a) Fr 2 and (b) Fr 1 from *V. cholerae* serotype O22. The spectra were recorded in  $\text{D}_2\text{O}$  at pH 7.0 and 295 K.

tion 1, and this signal was attributed to the methyl protons at position 6 of the 2-amino-2,6-dideoxy-D-glucose (QuiN) residue. This signal was absent from fraction 2 and suggested that fraction 2 probably corresponded to unsubstituted core oligosaccharide, whereas fraction 1 corresponded to substituted core oligosaccharide as 2-amino-2,6-dideoxy-D-glucose (QuiN) which is known to be a residue of the O-antigenic unit. These inferences were confirmed when the anomeric regions of the  $^1\text{H}$  NMR spectra of these two fractions were examined (Fig. 4).

The low-field region (4.40–6.0 ppm) of fraction 1 revealed eleven major signals. The resonances at ca. 5.00, ca. 4.70 and ca. 4.65 ppm could each be attributed to two protons. The  $^1\text{H}$  NMR spectrum of fraction 2 revealed seven major signals in the low-field region, the signal at ca. 5.20 ppm corresponding to two protons. The additional signals observed in the low-field region of fraction 1 were therefore assumed to originate from anomeric protons of the O-antigenic

unit of the LPS of this strain. This data therefore suggested that the O-antigenic unit of this strain consisted of six residues not including the 3,6-dideoxy-L-xylo-hexose residue(s) known to be present in this strain but presumed to have been lost on the derivatisation of this sample. This initial data therefore suggested that the O-antigenic unit from *V. cholerae* serotype O22 is larger than the O-antigenic unit from *V. cholerae* serotype O139.

The  $^1\text{H}$  NMR spectrum from fraction 1 of the backbone OS was assigned using COSY and TOCSY experiments (Table 1). The ring sizes and relative stereochemistries of the component monosaccharides were established from the  $^1\text{H}$  chemical shifts and the magnitude of the coupling constants [17]. However, overlap of signals at ca. 4.70 and ca. 4.65 ppm precluded complete assignment of these resonances. To completely assign these resonances, selective 3D NMR experiments were performed, utilising selective pulses and chemical-shift-selective filtration tech-

Table 1  
 $^1\text{H}$  NMR assignments for backbone LOS Fr1<sup>a</sup>

Sugar residue	H-1	H-2	H-3 eq ax	H-4	H-5	H6 a b	H-7 a b	H-8 a b	NOE inter only
A Hep	5.687	4.193	4.016	3.872	3.901	4.163	4.178		5.327 (B-1)
B Hep	5.327	3.924	3.874	nd <sup>b</sup>	nd	nd	3.963		3.989 (E-3)
C Hep	5.238	3.820	3.770	3.670	nd	nd	3.872		5.687 (A-1)
D Glc	5.203	3.577	3.824	3.535	3.748	nd	3.743		4.193 (A-2)
E Hep	5.125	4.150	3.989	4.099	4.255	4.101	nd		4.163 (A-6)
F GlcN	4.995	3.114	3.811	3.672	nd	nd			3.963 (A-7b)
G Glc	4.648	3.362	3.446	3.526	3.489	nd			4.101 (E-6)
H GlcN	4.492	2.752	3.426	3.590	3.470	nd			4.648 (G-1)
I GlcNoI	3.868 3.754	3.503	4.099	3.710	nd	nd			4.108 (Kdo-5)
Kdo			2.106 1.784	4.232	4.108	3.751	nd	nd	3.751 (Kdo-6)
U GalA	5.402	3.867	3.959	4.352	4.174				3.872 (B-7a)
V GlcN	5.026	3.057	3.841	4.142	3.620	nd			3.743 (B-7b)
W QuiN	4.707	3.817	3.675	3.455	3.550	1.338			4.099 (E-4)
X GalA	4.707	3.647	3.782	4.280	4.408				5.200 (D-1)
Y GalA	4.648	3.642	3.766	4.224	4.316				4.148 (I-6a)
Z GalA	4.567	3.642	3.752	4.232	4.107				3.796 (I-6b)

<sup>a</sup> Measured at 295 K, pH 7, from internal acetone (2.225 ppm).

<sup>b</sup> Not determined.

niques [18]. When these techniques were applied to the resonances at ca. 4.70 ppm in COSY–TOCSY experiments, separate subspectra were obtained after selective filtration of the well-resolved H-2 protons of each residue (Fig. 5). This experiment revealed that one of the resonances at ca. 4.70 ppm was the anomeric proton of a sugar with a *gluco*-configuration (W), and the second resonance belonged to the anomeric proton of a sugar with a *galacto*-configuration (X). The overlapping signals at ca. 4.65 ppm were also assigned in this way identifying a further *galacto*- and *gluco*-configured sugars.

Four  $^1\text{H}$  subspectra from fraction 1 were attributed to heptose residues (A, B, C, E) on the basis of their small  $J_{1,2}$  (ca. 1 Hz) and  $J_{2,3}$  (ca. 3 Hz) coupling constants, which pointed to pyranosyl ring systems of the *manno* configuration. A *cis* H-1–H-2 relationship ( $\alpha$ -D-configuration) was evident for all of these residues from the occurrence of a single residue NOE between the H-1 and H-2 resonances [19].

Large vicinal proton coupling constants for  $J_{2,3}$ ,  $J_{3,4}$  and  $J_{4,5}$  (8–10 Hz) indicated the presence of six hexopyranosyl residues having the *gluco*-configura-

tion (D, F, G, H, V, W). From the magnitude of the  $J_{1,2}$  couplings, three of these residues (G, H, W) were assigned to the  $\beta$ -D-configuration ( $J_{1,2}$  ca. 8 Hz), and the remaining three residues (D, F, V) were assigned to the  $\alpha$ -D-configuration ( $J_{1,2}$  ca. 4 Hz).

The residues F, H, V and W were identified as amino sugars on the basis of their C-2 chemical shifts. The H-2 resonances from these residues (3.114, 2.752, 3.057 and 3.817 ppm) were correlated in the HMQC experiment to the  $^{13}\text{C}$  resonances at 55.63, 57.47, 55.97 and 55.80 ppm, respectively, the chemical shifts being diagnostic of amino-substituted carbons. Residue W was subsequently identified as a 2-amino-2,6-dideoxy-D-glucopyranosyl residue (quinoxosamine), as the connectivity pathway for its anomeric proton led to a doublet at 1.338 ppm corresponding to the methyl protons at position 6. A fifth  $^{13}\text{C}$  resonance (56.51 ppm) in this region of the HMQC spectrum showed a correlation to a proton resonance at 3.503 ppm. The  $^1\text{H}$  spin system from this resonance was linked to two proton resonances H-1 and H-1' at 3.868 and 3.754 ppm, respectively. Indicative coupling constants of  $J_{1,1'} = 12$  Hz,  $J_{1,2} =$

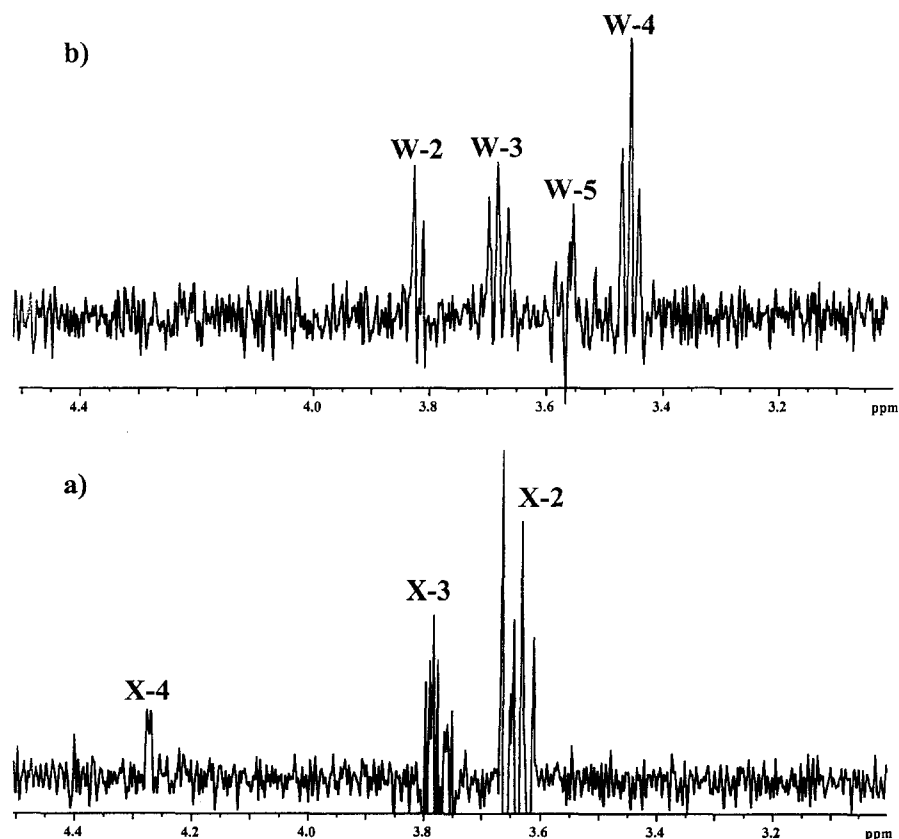


Fig. 5. 1D COSY–TOCSY spectra using selective excitation of H-1–W and H-1–X and chemical shift selective filtration through (a) H-2–X and (b) H-2–W. The spectra were recorded in  $\text{D}_2\text{O}$  at pH 7.0 and 295 K. The assignments of the resonances of the protons of residues W and X are indicated.

6 Hz and  $J_{1,2} = 7$  Hz for the glucosaminitol residue were observed, thus identifying the reduced glucosamine from lipid A [20].

Four subspectra having  $^1\text{H}$  spin systems typical of galacto-pyranosyl residues (U, X, Y, Z) were also identified from their vicinal ring proton coupling

constant values  $J_{2,3}$  (ca. 10 Hz),  $J_{3,4}$  (ca. 4 Hz) and  $J_{4,5}$  (1 Hz). From the magnitude of the  $J_{1,2}$  couplings, three of these residues (X, Y, Z) were assigned to the  $\beta$ -D-configuration ( $J_{1,2} = \text{ca. } 8$  Hz), and the remaining residue (U) was assigned to the  $\alpha$ -D-configuration ( $J_{1,2} = \text{ca. } 4$  Hz). As no galactose residues had been

Table 2

$^{13}\text{C}$  NMR assignments for backbone LOS Fr1<sup>a</sup>

Sugar residue	C-1	C-2	C-3	C-4	C-5	C-6	C-7
A Hep	99.41	80.12	71.05	nd <sup>b</sup>	nd	80.38	72.95
B Hep	102.26	72.91	81.66	nd	nd	nd	70.31
C Hep	99.63	72.33	nd	nd	nd	nd	nd
D Glc	102.60	73.13	nd	70.05	nd	nd	
E Hep	102.07	71.34	73.49	80.51	75.26	80.51	nd
F GlcN	98.60	55.63	nd	nd	nd	nd	
G Glc	103.71	75.10	77.45	nd	nd	nd	
H GlcN	104.07	57.47	77.45	nd	nd	nd	
I GlcNol	nd	56.51	67.21	nd	nd	nd	
Kdo	nd	nd	36.32	66.29	76.61	nd	nd
U GalA	101.41	72.11	70.37	80.67	72.62	nd	
V GlcN	100.58	55.97	74.17	73.36	nd	nd	
W QuiN	102.48	55.80	81.95	nd	nd	17.69	
X GalA	105.67	72.00	nd	70.34	75.97	nd	
Y GalA	104.10	73.82	nd	71.24	75.94	nd	
Z GalA	104.21	72.36	nd	69.73	76.13	nd	

<sup>a</sup> Measured at 295 K, pH 7, from internal acetone (31.07 ppm).

<sup>b</sup> Not determined. No assignments were made for C-8.

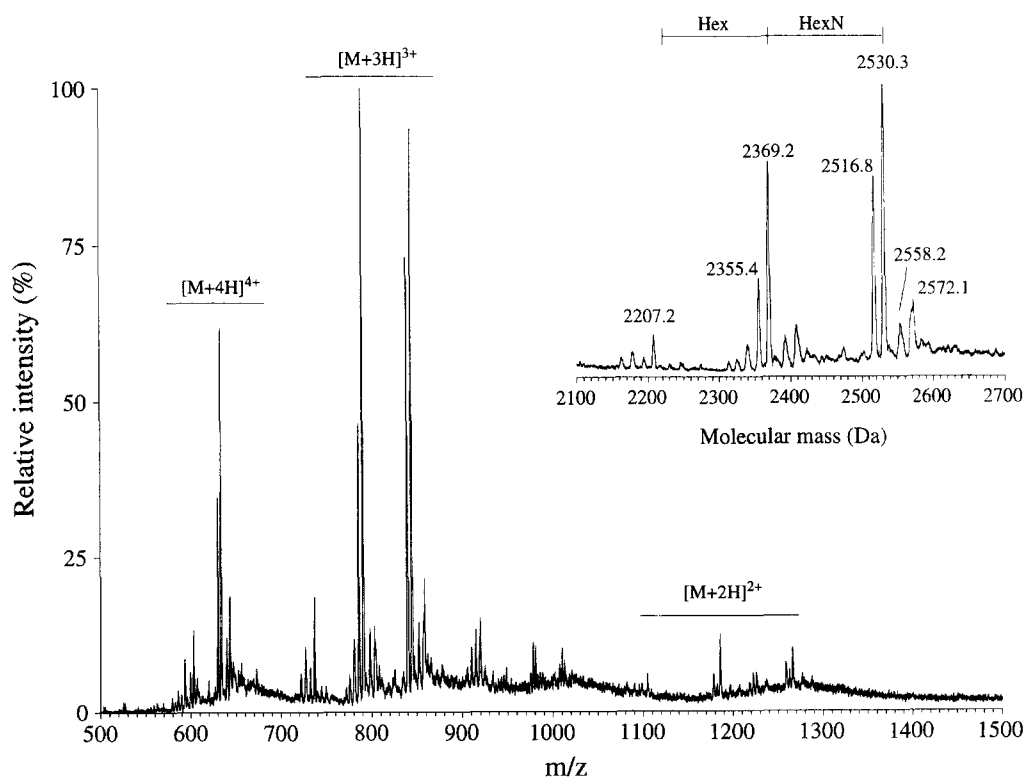


Fig. 6. Positive-ion ESIMS mass spectrum of the backbone OS fraction 1 from *V. cholerae* serotype O22.

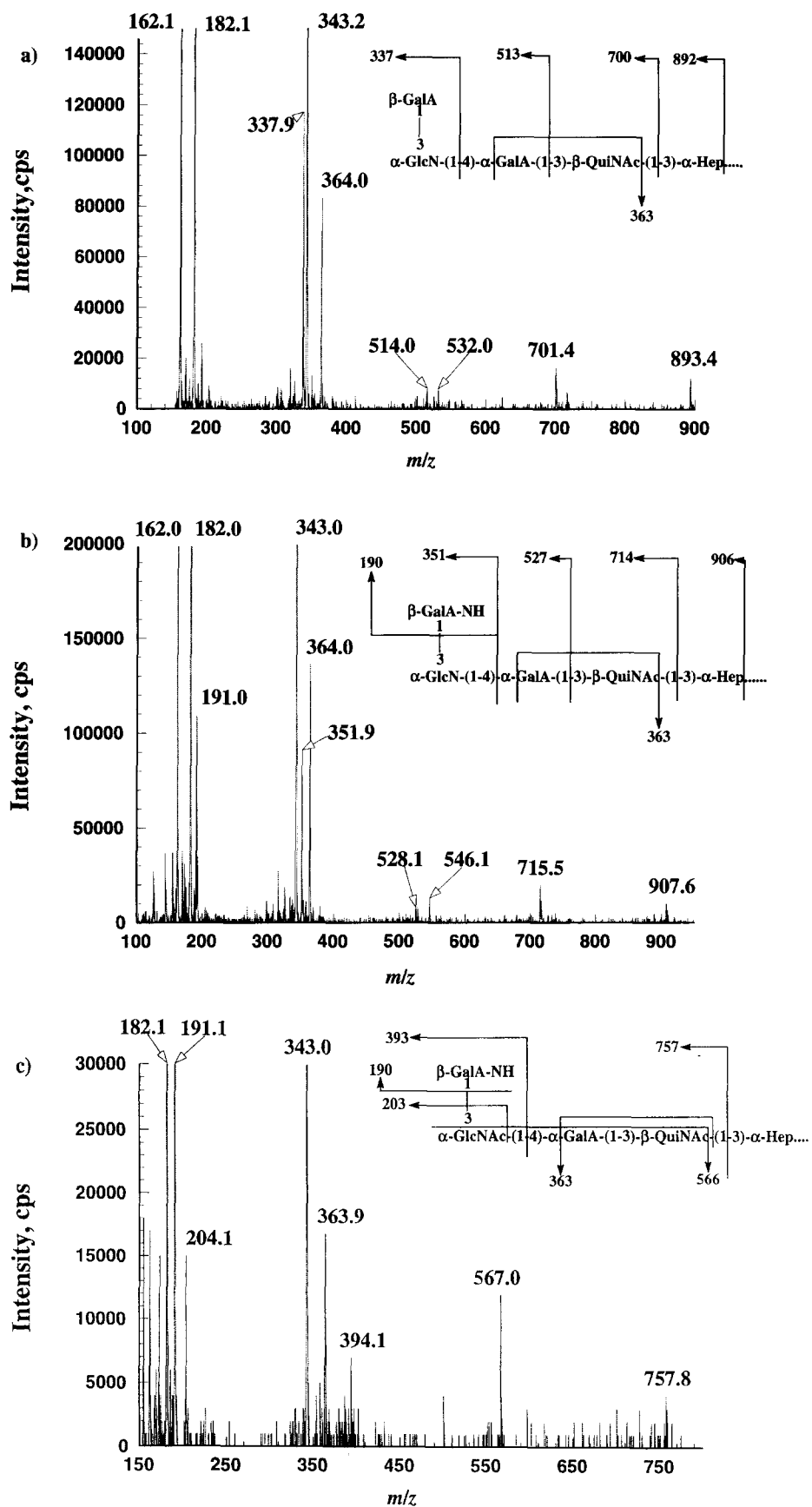


Fig. 7. Tandem mass spectral analyses of backbone OS from *V. cholerae*. Product ion spectra of  $[M + 3H]^{3+}$  ions at (a)  $m/z$  839.7, (b) 844.4, and (c) 858.4. Fragment ions appear as  $M + H^+$ .



identified in the derived alditol acetates, and studies on the KOH-treated sample had provided evidence for the presence of a galacturonic acid residue, it was postulated that the three other *galacto*-configured sugars were also uronic acids. This inference was confirmed when the derived alditol acetates and acetylated (*S*)-2-butyl glycosides were examined following carbodiimide reduction of the backbone OS. D-Galactose was now identified as a major constituent.

A subspectrum corresponding to the Kdo residue was identified from connectivity pathways that were accessed through the high-field H-3 resonances.

The sequence of glycosyl residues within fraction 1 of the backbone LOS was determined from inter-residue  $^1\text{H}$ – $^1\text{H}$  NOE measurements between anomeric and aglyconic protons on adjacent glycosyl residues. The linkage pattern for the repeating unit was determined in this way. Thus, the occurrence of an inter-residue NOE between H-1 of U and H-3 of W confirmed the partial sequence of  $\alpha$ -GalA-(1  $\rightarrow$  3)- $\beta$ -QuiN as determined for the KOH-treated sample. In addition, an interresidue NOE effect was observed between H-1 of V and H-4 of U. Interestingly, H-1 of X, Y and Z all gave interresidue NOE effects to H-3 of V. This result was initially confusing, but was clarified when the backbone-LOS sample was examined by mass spectrometry.

The anomeric configurations of the glycopyranosyl residues were confirmed from intraresidue NOE's relating the anomeric proton resonances to protons within the same pyranose ring systems. The  $\beta$ -linked glycopyranoses showed NOE's between H-1, H-3 and H-5 resonances within the same ring system, whereas the  $\alpha$ -linked sugars showed intraresidue NOE's between the anomeric proton and H-2 resonances, only.

Assignment of the  $^{13}\text{C}$  resonances was carried out by direct correlation of the  $^1\text{H}$  resonances in an HMQC experiment and by comparison of  $^{13}\text{C}$  resonances with similar chemical shift data (Table 2) [5–8,21,22].

The nanoelectrospray-ionization mass spectrum of the backbone OS fraction 1 gave a series of ions corresponding to the doubly and triply protonated molecules from which a reconstructed molecular mass profile was obtained (Fig. 6). The most prominent peaks were observed at  $m/z$  2369.2 and 2530.3. The difference of 161 amu between these molecular species was assumed to be due to the presence or absence of the terminal glucosamine residue of the outer core. The difference of 42 amu between molec-

ular species at 2530 and 2572 Da could be explained by incomplete N-deacylation; however, the 14 Da mass difference between 2516 and 2530 Da was confusing until the tandem MS–MS spectra were examined (Fig. 7). When the triply charged ion of  $m/z$  839.7 was examined by tandem MS–MS (Fig. 7a), fragment ions indicative of glucosamine ( $m/z$  162), glucosaminitol ( $m/z$  182) and lipidA ( $m/z$  343) were observed. Fragmentation from the non-reducing end of the molecule produced a variety of ions as shown. These fragments indicated that the quinovosamine residue had not been N-deacylated as evidenced by the presence of an internal fragment ion at  $m/z$  364 and of single glycosidic bond cleavage fragments at  $m/z$  701.4 and 893.4. However, when the triply charged ion of  $m/z$  844.4 was examined (Fig. 7b), significant differences were now observed in the fragmentation pattern of the non-reducing terminus. The terminal galacturonic acid residue had altered to form an oxonium fragment ion of  $m/z$  191. This difference clearly explains the observed difference of 14 amu in the nanoelectrospray mass spectrum Fig. 6. We tentatively suggest that the larger molecule is a hydrazide analog resulting from the prolonged treatment with hydrazine. When the triply charged ion of  $m/z$  858.4 was examined (Fig. 7c), a fragment ion at  $m/z$  204 was observed indicative of incomplete N-deacylation of the glucosamine residue. The presence of residues at the non-reducing termini that bear basic functionalities was clearly an advantage in obtaining abundant mass spectra. The MS–MS analysis confirmed the sequence of residues in the O-antigen as suggested by NMR spectroscopy and indeed identified a heptose residue as the point of attachment of the O-antigen to the core.

The presence of the three galacturonic acid residues (X, Y and Z) in the  $^1\text{H}$  NMR spectrum of fraction 1 can therefore be tentatively explained by the partial conversion of the uronic acid into a hydrazide, and the fact that the chemical environment of the anomeric proton of the substituting uronic acid will be different depending on whether the glucosamine residue is N-acetylated or not. Further evidence confirming the above inferences was obtained from an HMBC exper-

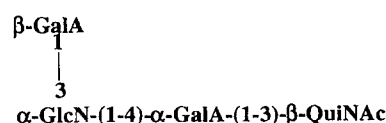


Fig. 8. Partial structure of the repeat unit of the backbone OS of *V. cholerae* O22.

Table 3

<sup>1</sup>H NMR assignments for delipidated sample Fr2<sup>a</sup>

Sugar residue	H-1	H-2	H-3 eq ax	H-4	H-5	H-6 a b	H-7 a b	H-8 a b	NOE inter only
A Hep	5.532	4.232	nd <sup>b</sup>	nd	nd	4.157	4.172 3.997		5.122 (B-1) 3.898 (E-3)
B Hep	5.122	4.054	nd	nd	nd	nd	3.970 3.616		5.532 (A-1) 4.232 (A-2)
C Hep	5.274	3.853	nd	nd	nd	nd	nd		4.157 (A-6) 3.997 (A-7b)
D Glc	5.193	3.565	nd	nd	nd	nd			4.175 (E-6) 4.629 (G-1)
E Hep	5.155	4.161	3.898	4.257	nd	4.175			3.636 (Kdo-?)
F GlcN	5.083	3.478	nd	nd	nd	nd			3.970 (B-7a) 3.616 (B-7b)
G Glc	4.629	3.231	3.477	3.130	3.388	nd			4.257 (E-4) 5.193 (D-1)
U GalA	5.408	3.943	3.946	4.373	4.300				3.653 (W-3)
V GlcN	4.867	3.872	4.134	3.621	4.237	nd			4.373 (U-4)
W QuiN	4.677	3.753	3.653	3.448	3.548	1.330			4.054 (B-2) 4.100 (B-3)
X GalA	4.780	3.865	5.106	4.418	4.355				4.134 (V-3)
X' GalA	4.780	3.592	4.116	5.620	4.334				4.134 (V-3)
X'' GalA	4.657	3.666	3.915	4.234	4.300				4.134 (V-3)
X''' GalA	4.730	3.666	4.135	5.588	4.336				4.134 (V-3)
S Col	5.057	3.983	1.922 1.782	3.748	4.114	1.146			3.666 (X'-2) and (X'''-2)
T Col	4.963	3.915	1.900 1.752	3.728	4.172	1.156			3.865 (X-2)

<sup>a</sup> Measured at 295 K, pH 7, from internal acetone (2.225 ppm).<sup>b</sup> Not determined.

iment that revealed that the proton resonances from Y1 and Z1 were linked to the carbon resonance of V3. Hence the partial sequence from the repeating unit portion of the backbone OS from fraction 1 was established and is shown in Fig. 8.

Assignment of the <sup>1</sup>H NMR spectrum of fraction 2 backbone OS was achieved by utilising similar methods as described for fraction 1. This analysis readily confirmed fraction 2 as the unsubstituted core-lipid A region of the LOS.

Comparison of the O-antigenic unit structures from *V. cholerae* serotypes O139 and O22 reveals the same linkage from glucosamine to the galacturonic acid [6]. However, in serotype O22 the amino sugar has the α-configuration, whereas in O139 it was in the β-configuration. Also, instead of galactose attached to the 3-position of the glucosamine as is the case for O139, in serotype O22 a galacturonic acid residue is attached.

The serological relatedness of these strains was more clearly understood when the delipidated sample of *V. cholerae* serotype O22 was studied.

Gel-filtration chromatography of the delipidated mixture resulted in three fractions. Fraction 1 was assumed to correspond to unhydrolysed LOS from its cloudy appearance and was not studied further.

Examination of fraction 2 by <sup>31</sup>P NMR spectroscopy revealed that there were no phosphate

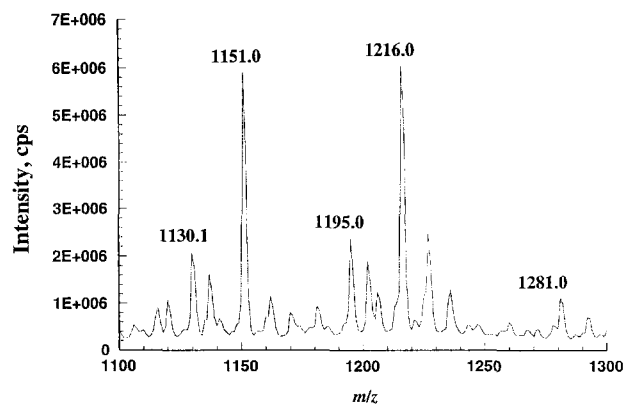


Fig. 9. Doubly charged region of the positive-ion ESIMS mass spectrum of the delipidated LPS fraction 2 from *V. cholerae* serotype O22.

residues present, and hence the cyclic phosphate residue in serotype O139 LOS is absent from the LOS of serotype O22.

When the  $^1\text{H}$  NMR spectrum was examined, it confirmed and extended the earlier data. Assignments are listed in Table 3. This sample was heterogeneous due to the partial loss of the 3,6-dideoxy-L-xylo-hexose residues on delipidation and also due to the identification of non-stoichiometrically attached O-acetyl groups. Two residues (S and T) of 3,6-dideoxy-L-xylo-hexose were identified. Characteristic signals for the H-3 methylene protons were observed at 1.922 (eq) and 1.782 ppm (ax) for S and at 1.900 (eq)

and at 1.752 ppm (ax) for T. Signals indicative of the protons of the methyl groups at H-6 were also observed at 1.146 ppm for S and at 1.156 ppm for T. On closer examination of the  $^1\text{H}$  NMR spectrum of the delipidated sample, four additional signals in the anomeric region were observed at 5.620, 5.588, 5.106 and 5.133 ppm that in a  $^{13}\text{C}$ - $^1\text{H}$  HMQC spectrum correlated with  $^{13}\text{C}$  coordinates of 73.28, 73.60, 76.40 and 71.64 ppm, suggesting these signals were shifted to low field due to the presence of O-acetyl substituents. Examination of the COSY and TOCSY experiments permitted the assignment of three of these resonances. The signals at 5.620 and at 5.588

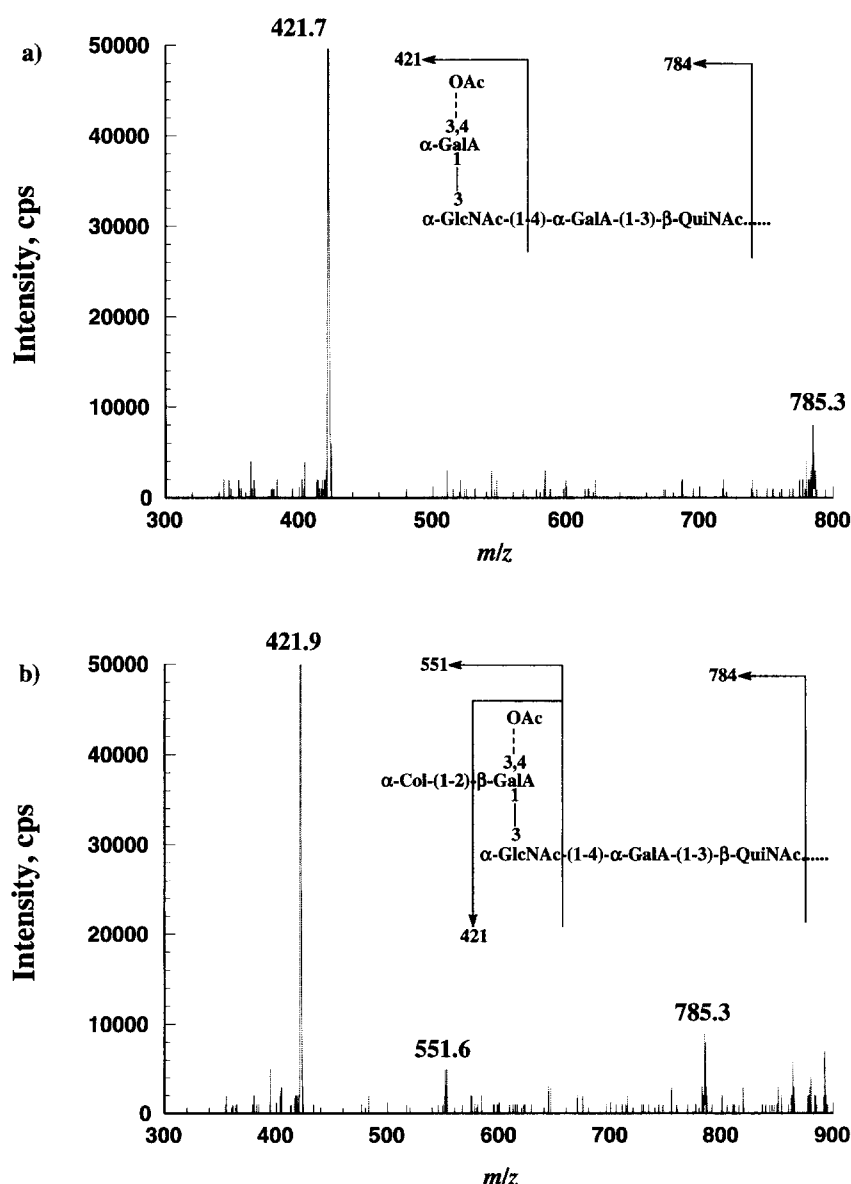


Fig. 10. Tandem mass spectral analyses of fraction 2 of the delipidated LPS from *V. cholerae* serotype O22. Product ion spectra of  $[\text{M} + 2\text{H}]^{2+}$  ions at (a)  $m/z$  1151.3 and (b) 1216.0. Fragment ions appear as  $\text{M} + \text{H}^+$ .

ppm were assigned to H-4 of the galacturonic acid residues (X' and X''), and the signal at 5.106 ppm was assigned to H-3 of the galacturonic acid residue (X). However, these signals were not found to be in the same spin-system, suggesting that the galacturonic acid (X) is either acetylated at the 3- or 4-position, but not at both positions simultaneously. The presence or absence of the 3,6-dideoxy-L-xylo-hexose residue also contributed to the various assignments of the galacturonic acid residue (X). Galacturonic acid

residue (X'') was not O-acetylated. The signal at 5.133 ppm could not be assigned at this stage.

The sites of attachment of the 3,6-dideoxy-L-xylo-hexose residues were determined in a NOESY experiment. Interresidue NOEs between H-1 of S and H-2 of X'' (3.666) and X''' (3.666), and between H-1 of T and H-2 of X (3.865 ppm) were observed identifying both 3,6-dideoxy-L-xylo-hexose residues as the same terminal sugar, its assignment differing depending on the position and presence of the O-acetyl residues on

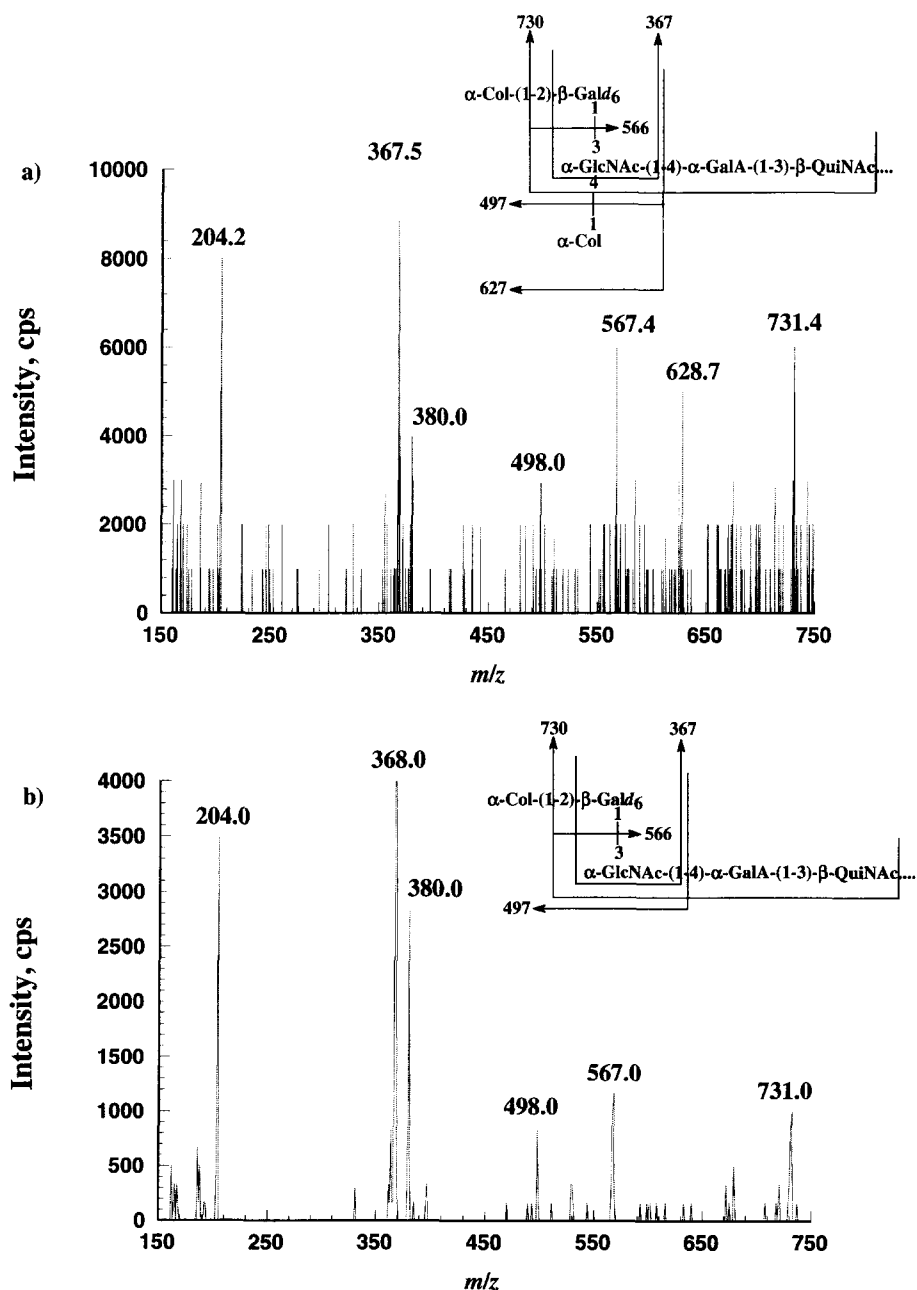


Fig. 11. Tandem mass spectral analyses of fraction 2 of the carbodiimide reduced, delipidated LPS from *V. cholerae* serotype O22. Product ion spectra of  $[M + 2H]^{2+}$  ions at (a)  $m/z$  1235.0 and (b) 1170.0. Fragment ions appear as  $M + H^+$ .

the galacturonic acid residue. Interestingly the 3,6-dideoxy-L-xylo-hexose residue T was only found to be attached to X when X was acetylated at the 3-position. The absence of an interresidue NOE between the 3,6-dideoxy-L-xylo-hexose residues and galacturonic acid residue X' suggested that this residue was unsubstituted due to losses of the 3,6-dideoxy-L-xylo-hexose residues on delipidation. Interestingly no interresidue NOEs were observed to suggest substitution of the N-acetylated-glucosamine residue (V) with a 3,6-dideoxy-L-xylo-hexose residue. This result suggests that this 3,6-dideoxy-L-xylo-hexose residue was almost completely lost on delipidation. However, evidence for attachment of a 3,6-dideoxy-L-xylo-hexose residue to the 2-acetamido-2-deoxy-D-glucose (N-acetylglucosamine) residue (V) was obtained by nanoelectrospray-ionization MS analysis as described below.

Mass spectrometric analysis of the delipidated sample confirmed and extended the NMR data. Methylation analysis of fraction 2 confirmed all the linkages of the core region. However, the methylated, delipidated oligosaccharide upon hydrolysis with formic and sulfuric acid did not lead to quantitative release of any of the O-antigenic unit residues, indicating the relative resistance of the uronic acid and amino sugar linkages and degradation of the 3,6-dideoxy-L-xylo-hexose residues. Methylation analysis following carbodiimide reduction, however, now suggested the presence of 2-substituted and terminal Gal(*d*<sub>6</sub>) (arising from sodium borodeuteride reduction) and also evidence for 3,4-disubstituted GlcNAc and 3-substituted QuiNAc. The failure of carbodiimide reduction at reducing the 4-substituted

galacturonic acid residue can be tentatively explained by steric factors as the more accessible and indeed sometimes terminal galacturonic acid residue was clearly reduced. These results were confirmed by mass spectrometric analysis (see below).

Nanoelectrospray-ionization mass spectral analysis of fraction 2 in positive-ion mode showed a number of multiply charged ions from which a molecular mass profile was derived (Fig. 9). The presence of oligosaccharides of molecular masses of 2560, 2430 and 2300 Da were in excellent agreement with the expected structure and indicative of partial and complete loss of the two 3,6-dideoxy-L-xylo-hexose residues on delipidation as implicated by the <sup>1</sup>H NMR data. Tandem MS–MS analysis of the doubly charged region of fraction 2 confirmed the structural inferences from the nanoelectrospray spectrum. The product-ion spectrum of *m/z* 1151.0 (Fig. 10a) showed an abundant fragment ion at *m/z* 421.7, indicative of complete loss of 3,6-dideoxy-L-xylo-hexose and presence of an O-acetyl group. When the doubly charged ion of *m/z* 1216.0 was examined (Fig. 10b) a peak at *m/z* 551.6 was obtained indicative of partial loss of one of the 3,6-dideoxy-L-xylo-hexose residues and presence of an O-acetyl group. The presence of a peak of *m/z* 421.7 in Fig. 10b can be explained by loss of the 3,6-dideoxy-L-xylo-hexose residue during the MS–MS analysis. When the carbodiimide-reduced derivative of delipidated fraction 2 was examined by tandem MS–MS, product spectra (Fig. 11a and b) were obtained indicative of partial loss of 3,6-dideoxy-L-xylo-hexose and failure to reduce the 4-substituted galacturonic acid residue. This result when considered in conjunction with the

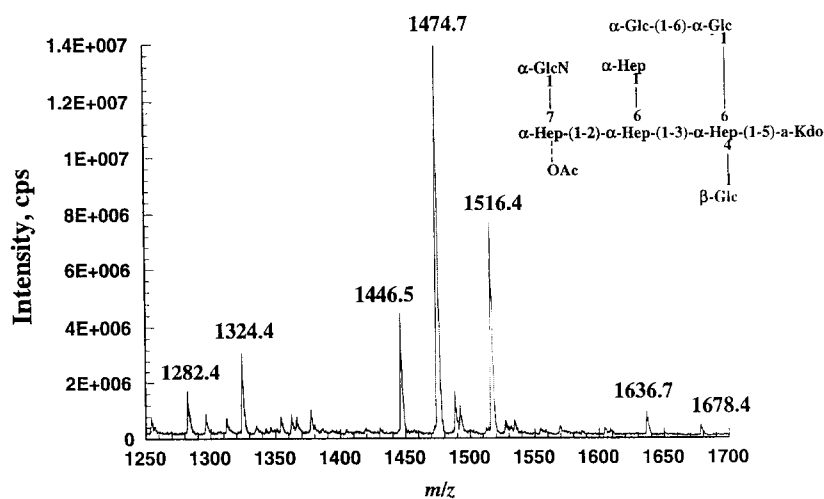


Fig. 12. Positive-ion ESIMS mass spectrum of fraction 3 of the delipidated LPS from *V. cholerae* serotype O22.

methylation analysis data on this sample suggests that the 3,6-dideoxy-L-xylo-hexose residue substitutes the *N*-acetylglucosamine residue (V) at the 4-position.

Fraction 3 of the delipidated material was confirmed as the unsubstituted core region when the nanoelectrospray-ionization mass spectrum was examined (Fig. 12). The most prominent peaks at  $m/z$  1474.7 and 1516.4 were indicative of the presence of an acetyl group due to their 42 Da mass differential.

The basic composition of these ions is (Hep)<sub>4</sub>, (Glc)<sub>2</sub>, GlcN and an anhydro-Kdo derivative (202 Da) formed on acid hydrolysis [23–25]. Small peaks indicative of the (Glc)<sub>3</sub> containing molecules were observed at  $m/z$  1636.7 and 1678.4.

Tandem MS–MS analysis (Fig. 13a and b) of fraction 3 enabled the identification of the residue to which the acetyl group is attached. As illustrated in Fig. 13a, when the non-acetylated molecule at  $m/z$

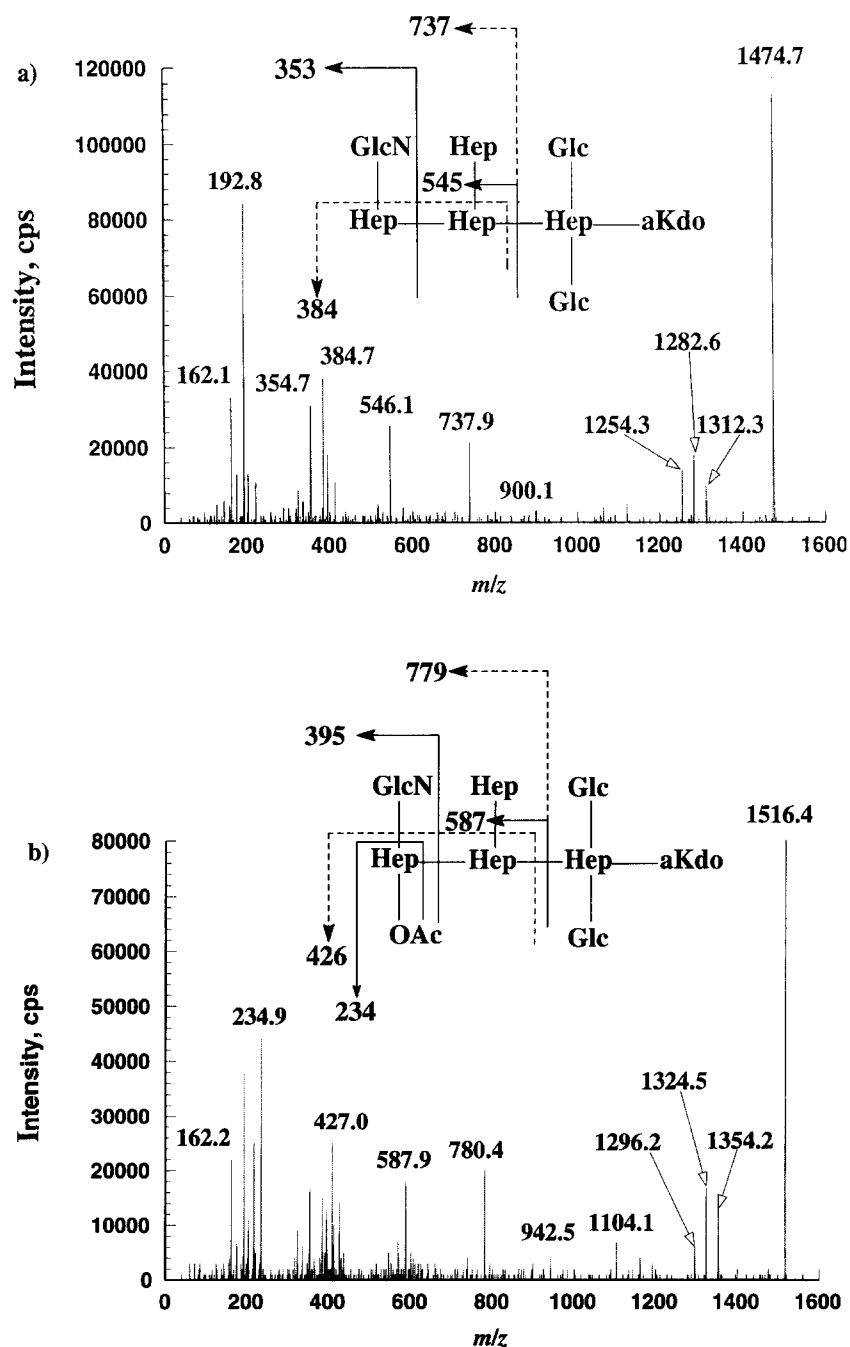


Fig. 13. Tandem mass spectral analyses of fraction 3 of the delipidated LPS from *V. cholerae* serotype O22. Product ion spectra of  $[M + H]^+$  ions at (a)  $m/z$  1474.7 and (b) 1516.4. Fragment ions appear as  $M + H^+$ .

1474.7 was subjected to MS–MS, fragment ions were observed at  $m/z$  192.8, 354.7, 384.7, 546.1, 737.9 and 900.1. When the acetylated molecule at  $m/z$  1516.4 was examined, the corresponding fragment ions appeared at  $m/z$  234.9, 395.9, 427, 587.9, 780.4 and 942.5 (Fig. 13b). These results clearly localise the acetyl group to the outermost heptose residue of the core region. This data therefore also provide an explanation for the previously unassigned ‘non-anomeric’ NMR signals at 5.133, 71.64 ppm. Unfortunately, insufficient amounts of fraction 3 precluded an NMR analysis.

### 3. Discussion

The structural elucidation of the LPS from *V. cholerae* serotype O22 confirms the serological observations that serotypes O139 and O22 share a common epitope, but also possess unique epitopes (Fig. 14).

Both serotypes contain the same trisaccharide GlcNAc–GalA–QuiNAc, and in both cases the *N*-acetylglucosamine is disubstituted at the 3- and 4-positions. However, in serotype O22 the *N*-acetylglucosamine has the  $\alpha$ -configuration and not the  $\beta$ -configuration observed previously for O139. The substituent at the 3-position also differs, being a galacturonic acid residue in O22 and a cyclic phosphorylated galactose in serotype O139. It is noteworthy

that the phosphate group is absent in serotype O22 as such groups are often found to be immunodominant. It is also interesting to note that the rare terminal 3,6-dideoxy-*L*-xylo-hexose residues are also present both in serotype O22 and in serotype O139.

The striking structural similarity between serotypes O22 and O139, therefore, adds to the existing data suggesting that serotype O22 was the donor strain of the new genetic material forming the new O139 serotype. This structural evidence, when considered in conjunction with the facts that serotypes O22 and O139 are the only cholera strains to produce colitose and that significant homology has been found between genes of the *rfb* clusters of serotypes O139 and O22 [14], makes it very likely that serotype O22 was the progenitor strain.

However, structural differences do exist between these two serotypes, the most striking examples being the lack of a cyclic phosphate group and the lack of capsular material in serotype O22. The change in the anomeric configuration of the *N*-acetylglucosamine and the conversion of galactose to galacturonic acid must also be explained genetically if O22 was the donor strain. A recent paper [26] has shown that additional genes outside the ‘*rfb*’ cluster are essential for O-antigen biosynthesis in *V. cholerae* serotype O1. These genes are therefore still present in serotype O139, and these gene products would be able to modify the structure produced by the ‘new *rfb*’ clus-

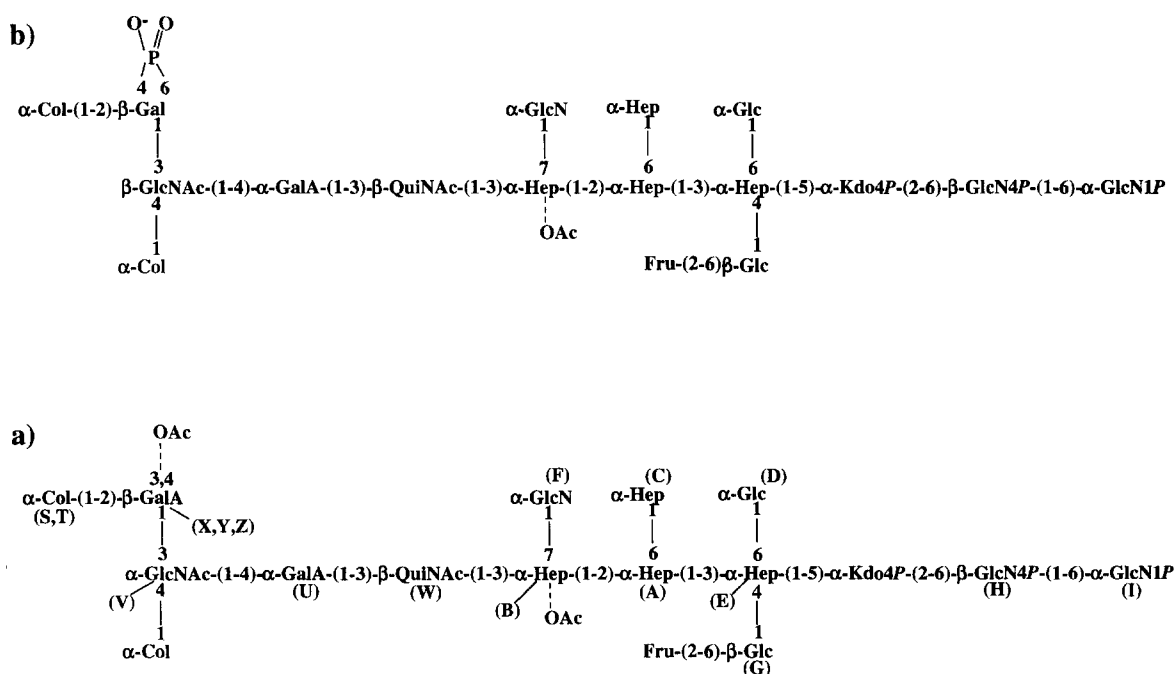


Fig. 14. Chemical structure of the LPS of (a) *V. cholerae* O22 and (b) *V. cholerae* O139.

ter'. Such a mechanism provides a possible explanation for the structural differences observed between *V. cholerae* O22 and O139 lipopolysaccharides.

Other bacterial strains also possess repeat unit structures of considerable similarity to *V. cholerae* serotypes O139 and O22, including *Aeromonas trota* [27] and *Salmonella greenside* [28]. Although structurally different from serotype O139, the significant similarities between these strains suggest that the DNA clusters responsible for the LPS biosynthesis of these strains are possibly evolutionarily linked.

During the elucidation of this structure, it became apparent that two errors were made in the structural elucidation of serotype O139 [5,6]. Residue E in the KOH-treated sample [5] and residue C in the delipidated sample [6] were misidentified as glucose residues, when in fact they were the terminal heptose residue. Also the point of attachment of the O-antigenic repeat unit to the core region was incorrectly assigned to the 2-position of a heptose residue. Inter-residue NOE measurements were observed from the quinovosamine residue to both the 2- and 3-positions of the heptose residue. However, by utilisation of Metropolis Monte Carlo (MMC) [29] methods, the point of attachment was unambiguously assigned as the 3-position. The presence of an O-acetyl group in the core region of the *V. cholerae* serotype O139 LPS was also overlooked; however, closer examination of the nanoelectrospray-ionization mass spectrum of the delipidated LPS of fraction 2 from serotype O139 (Fig. 1, Ref. [6]), revealed that an O-acetyl group is also present in the core region of this serotype.

#### 4. Experimental

**Isolation of lipopolysaccharide.**—*V. cholerae* serotype O22 (NRCC #4904) was grown in BHI with 1% NaCl at 37 °C for 17 h. Cells were harvested by centrifugation ( $10000 \times g$ ). LPS was isolated by the aqueous phenol method [15].

**Purification of lipopolysaccharide.**—LPS was deacylated by treatment with 4 M KOH (ca. 4 mL per 50 mg) at 120 °C for 16 h [30]. The solution was cooled, neutralised and centrifuged. The supernatant solution was lyophilised, and the resulting lipooligosaccharide was purified by gel-filtration chromatography on a Sephadex G-10 column eluted with pyridinium acetate (0.05 M, pH 4.5). Column eluents were monitored for changes in refractive in-

dex, and collected fractions (4.5 mL) were assayed colorimetrically for neutral glycoses [31].

LPS was delipidated according to the following procedure. LPS (440 mg) was hydrolysed at 100 °C for 4 h at pH 4.2 in a solution of 0.1 M sodium acetate (50 mL). Insoluble material was removed by centrifugation, the supernatant solution was lyophilised, and the resulting oligosaccharide was purified by Sephadex G-10 gel-filtration column chromatography. Column eluents were monitored for changes in refractive index, and collected fractions (4.5 mL) were assayed colorimetrically for neutral glycoses. This desalted product was re-hydrolysed and desalted as above and then was further purified by gel-filtration chromatography on a Bio-Gel P2 column, monitoring column eluents as above.

Deacylated, dephosphorylated and reduced LPS (backbone) was prepared according to a modified method by Masoud et al. [20] of that reported by Holst et al. [32]. LPS (160 mg) was treated with anhydrous hydrazine (15 mL) with stirring at 37 °C for 30 min. The reaction was cooled (0 °C), cold acetone (−70 °C, 50 mL) was added gradually to destroy excess hydrazine, and precipitated O-deacylated LPS was obtained by centrifugation. O-Deacylated LPS was dephosphorylated by treatment with 48% aqueous hydrogen fluoride (10 mL) at 0 °C for 48 h. The product was dialysed against water, and the O-deacylated, dephosphorylated LPS sample was reduced ( $\text{NaBH}_4$ , 100 mg, 22 °C, 1 h), and excess  $\text{NaBH}_4$  was removed by dialysis following neutralisation. O-Deacylated, dephosphorylated and reduced LPS was dried over phosphorus pentoxide and treated with anhydrous hydrazine (8 mL, 85 °C, 7 days) to remove amide-linked fatty acids. After removal of hydrazine in vacuo over sulfuric acid, the backbone oligosaccharide was redissolved, lyophilised, and the product purified on a Bio-Gel P-2 column monitoring column eluents as above.

**DOC–PAGE analysis.**—Polyacrylamide gel electrophoresis (PAGE) was performed by using the system of Laemmli and Favre [33] as modified by Komuro and Galanos [34] with deoxycholate (DOC) as the detergent. The separation gel contained final concentrations of 13% acrylamide, 0.5% DOC and 375 mM Tris–HCl (pH 8.8), with the stacking gel containing 4% acrylamide, 0.5% DOC and 125 mM Tris–HCl (pH 6.8). LPS samples were prepared at a concentration of 0.1% (w/v) in the sample buffer (0.25% DOC, 175 mM Tris–HCl [pH 6.8], 10% glycerol). Bromophenol blue (0.002% in sample buffer) was used as the tracking dye. The electrode



buffer (pH 8.4) was composed of DOC ( $2.5 \text{ gL}^{-1}$ ), glycine ( $14.4 \text{ gL}^{-1}$ ) and Tris ( $3.0 \text{ gL}^{-1}$ ). Electrophoresis was performed at a constant current of 30 mA. Gels were fixed in an aqueous solution of 40% ethanol and 5% acetic acid. LPS bands were stained and visualised by silver staining as described by Tsai and Frasch [35].

**Analytical methods.**—Glycoses were determined by GLC–MS as their alditol acetate derivatives [36]. Samples ( $0.5\text{--}1.0 \text{ mg}$ ) were hydrolysed with either 2 M TFA for 90 min at  $125^\circ\text{C}$ , or by mild conditions with  $0.02 \text{ M H}_2\text{SO}_4$  for 30 min at  $100^\circ\text{C}$ . The liberated glycoses were reduced ( $\text{NaBH}_4$ ) and acetylated ( $\text{Ac}_2\text{O}$ ) [37]. The absolute configurations of the LPS components were identified by GLC analysis of their acetylated (*S*)-2-butyl glycosides [36]. Carbodiimide reduction was carried out according to the method employed by Sadovskaya et al. [38].

**Methylation analysis.**—Oligosaccharide samples ( $2\text{--}4 \text{ mg}$ ) were methylated with iodomethane in dimethyl sulfoxide containing an excess of potassium (methylsulfinyl)methanide [39]. The methylated oligosaccharides were purified on a Sep-Pak  $\text{C}_{18}$  cartridge [40]. The purified methylated oligosaccharides were hydrolysed by initial treatment with 90% (v/v) formic acid at  $100^\circ\text{C}$  for 1 h, followed by overnight treatment with  $0.13 \text{ M H}_2\text{SO}_4$  at  $100^\circ\text{C}$ . Hydrolysis products were then reduced ( $\text{NaBD}_4$ ), acetylated, and analysed by GLC–MS.

**Mass spectrometry.**—All mass spectrometric experiments were conducted using an API 300 triple quadrupole mass spectrometer (Perkin–Elmer/SCIEX, Concord, Ont., Canada). Nanoelectrospray-ionization mass spectra were obtained using a modified MicroIonSpray interface (PE/SCIEX) comprising a small tee insert used to establish electrical contact between a fused silica transfer line ( $80 \text{ cm} \times 50 \text{ }\mu\text{m}$  i.d.) and the emitter tip. Disposable nanoelectrospray emitters were made of small length of tapered fused silica ( $5.3 \text{ cm} \times 50 \text{ }\mu\text{m}$  i.d. with a  $5 \text{ }\mu\text{m}$  tip diameter) prepared in a similar manner to that described previously [41]. Samples (approximately  $0.1 \text{ mg mL}^{-1}$  in  $0.1 \text{ M HCOOH}$ ) were infused to the mass spectrometer at a flow rate of approximately  $200 \text{ nL min}^{-1}$  using a pressurized inlet device.

Conventional mass spectra were typically acquired over the range  $m/z$  400–1800 using 1 ms dwell time period per  $0.1 m/z$  unit step. Tandem mass spectrometry experiments were conducted using identical conditions to that described above except that precursor

ion were selected by the first quadrupole (Q1) while the third quadrupole (Q3) was scanned over the desired mass range to collect fragment ions formed in the r.f.-only quadrupole collision cell. Collisional activation was performed using nitrogen collision gas at an energy of typically 75 eV in the laboratory frame of reference. Tandem mass spectra were acquired using dwell times of 0.5 ms per step of  $0.1 \text{ Da}$  in full-scan mode.

**NMR spectroscopy.**—NMR spectra were obtained on a Bruker AMX 500 or AMX 600 spectrometer using standard Bruker software. Measurements were made at 295 K at concentrations ca.  $10 \text{ mg mL}^{-1}$  in  $\text{D}_2\text{O}$ , subsequent to several lyophilisations with  $\text{D}_2\text{O}$ .

1D  $^1\text{H}$  NMR spectra were measured at 600.14 MHz using a spectral width of 6.0 kHz. Acetone was used as an internal standard, and chemical shifts were referenced to the methyl resonance ( $\delta_{\text{H}} = 2.225 \text{ ppm}$ ;  $\delta_{\text{C}} = 31.07 \text{ ppm}$ ). 2D homonuclear proton correlation experiments (COSY), total correlation experiments (TOCSY) and nuclear Overhauser effect experiments (NOESY) were measured over a spectral width of 3.62 kHz, using data sets ( $t_1 \times t_2$ ) of  $4096 \times 1024$ , and 16 scans were acquired. Mixing times of 200 ms was employed for the NOESY experiments.

Heteronuclear 2D  $^{13}\text{C}$ – $^1\text{H}$  chemical shift correlations were measured in the  $^1\text{H}$ -detected mode via multiple quantum coherence (HMQC) with proton decoupling in the  $^{13}\text{C}$  domain, using data sets of  $2048 \times 512$  points and spectral widths of 4.24 and 16.6 kHz for  $^1\text{H}$  and  $^{13}\text{C}$  domains respectively. A total of 64 scans were acquired for each  $t_1$  value.

$^{31}\text{P}$  NMR spectra were measured at 202.5 MHz by employing spectral widths of 41.6 kHz and phosphoric acid (85%) was used as the external standard ( $\delta_{\text{P}} = 0.0 \text{ ppm}$ ).  $^{31}\text{P}$ – $^1\text{H}$  correlations (HMQC) were made in the  $^1\text{H}$ -detected mode by using a data matrix of  $2048 \times 128$  points, sweep widths of 2 kHz for  $^{31}\text{P}$  and 4.5 kHz for  $^1\text{H}$ , and a delay of 60 ms.

To fully assign the spectra selective 1D TOCSY, 1D NOESY and 1D analogues of 3D NOESY–TOCSY and TOCSY–NOESY experiments [42] were performed using a  $270^\circ$  Gaussian pulse (1024 points) truncated at 2.5% for selective excitation. The pulse width of the selective pulses was 50–80 ms. Spin-lock mixing times for the TOCSY varied from 20 to 80 ms. The NOESY mixing time was 200 ms. Due to overlap of some of the anomeric signals, it was necessary to utilise further selective 3D experiments that employed chemical-shift-selective filter (CSSF) techniques [18].

## Acknowledgements

We thank Dr. T. Shimada (NIH, Japan) for the *V. cholerae* serotype O22 culture, D.W. Griffith for cell growth, and D. Krajcarski and R. Johnson for mass spectrometry.

## References

- [1] M.J. Albert, A.K. Siddique, M.S. Islam, A.S.G. Faruque, M. Ansaruzzuman, S.M. Faruque, and R.B. Sack, *Lancet*, 341 (1993) 704.
- [2] E.M. Bik, A.E. Bunschoten, R.D. Gouw, and F.R. Mooi, *EMBO J.*, 14 (1995) 209–216.
- [3] L.E. Comstock, J.A. Johnson, J.M. Michalski, J.G. Morris, Jr., and J.B. Kaper, *Mol. Microbiol.*, 19 (1996) 815–826.
- [4] U.H. Stroeher, G. Parasivam, B.K. Dredge, and P.A. Manning, *J. Bacteriol.*, 179 (1997) 2740–2747.
- [5] A.D. Cox, J.-R. Brisson, V. Varma, and M.B. Perry, *Carbohydr. Res.*, 290 (1996) 43–58.
- [6] A.D. Cox and M.B. Perry, *Carbohydr. Res.*, 290 (1996) 59–65.
- [7] L.M. Preston, Q. Zu, J.A. Johnson, A. Joseph, D.R. Maneval, K. Hussain, G.P. Reddy, C.A. Bush, and J.G. Morris, *J. Bacteriol.*, 177 (1995) 835–838.
- [8] Y.A. Knirel, L. Parades, P.-E. Jansson, A. Weintraub, G. Widmalm, and M.J. Albert, *Eur. J. Biochem.*, 232 (1995) 391–396.
- [9] E.M. Bik, A.E. Bunschoten, R.D. Gouw, and F.R. Mooi, *EMBO J.*, 14 (1995) 209–216.
- [10] E.M. Bik, A.E. Bunschoten, R.J.L. Willems, A.C.Y. Chang, and F.R. Mooi, *Mol. Microbiol.*, 20 (1996) 799–811.
- [11] T. Shimada, E. Arakawa, K. Itoh, T. Nakazato, T. Okitsu, S. Yamai, M. Kusum, G.B. Nair, and Y. Takeda, *Curr. Microbiol.*, 29 (1994) 331–333.
- [12] Y. Isshiki, S. Kondo, T. Iguchi, Y. Sano, T. Shimada, and K. Hisatsune, *Microbiology*, 142 (1996) 1499–1504.
- [13] S. Kondo, Y. Kawamata, Y. Sano, T. Iguchi, and K. Hisatsune, *System. Appl. Microbiol.*, 20 (1997) 1–11.
- [14] S. Vimont, S. Dumontier, V. Escuyer, and P. Berche, *Gene*, 185 (1997) 43–47.
- [15] K.G. Johnson and M.B. Perry, *Can. J. Microbiol.*, 22 (1976) 29–34.
- [16] F.M. Unger, *Adv. Carbohydr. Chem. Biochem.*, 38 (1981) 323–388.
- [17] C. Altona and C.A.G. Haasnoot, *J. Org. Magn. Reson.*, 13 (1980) 417–429.
- [18] D. Uhrin, J.-R. Brisson, and D.R. Bundle, *J. Biomol. NMR*, 3 (1993) 367–373.
- [19] J.C. Richards and M.B. Perry, *Biochem. Cell Biol.*, 66 (1988) 758–771.
- [20] H. Masoud, M.B. Perry, J.-R. Brisson, D. Uhrin, and J.C. Richards, *Can. J. Chem.*, 72 (1994) 1466–1477.
- [21] K. Bock and C. Pederson, *Adv. Carbohydr. Chem. Biochem.*, 41 (1983) 27–66.
- [22] K. Bock, C. Pederson, and H. Pederson, *Adv. Carbohydr. Chem. Biochem.*, 42 (1984) 193–225.
- [23] D. Charon and L. Szabo, *J. Chem. Soc., Perkin Trans. 1*, (1973) 1175–1179.
- [24] P.A. McNicholas, M. Batley, and J.W. Redmond, *Carbohydr. Res.*, 165 (1987) 17–22.
- [25] L.D. Melton, E.R. Morris, D.A. Rees, D. Thom, and S.M. Bocick, *Carbohydr. Res.*, 81 (1980) 295–303.
- [26] A. Fallarino, C. Mavrangelos, U.H. Stroeher, and P.A. Manning, *J. Bacteriol.*, 179 (1997) 2147–2153.
- [27] Y.A. Knirel, S.N. Senchenkova, P.-E. Jansson, A. Weintraub, M. Ansaaruzzaman, and M.J. Albert, *Eur. J. Biochem.*, 238 (1996) 160–165.
- [28] L. Kenne, B. Lindberg, E. Soderholm, D.R. Bundle, and D.W. Griffith, *Carbohydr. Res.*, 111 (1983) 289–296.
- [29] T. Peters, B. Meyer, R. Stuike-Prill, R. Somorjai, and J.-R. Brisson, *Carbohydr. Res.*, 238 (1993) 49–73.
- [30] O. Holst, J.E. Thomas-Oates, and H. Brade, *Eur. J. Biochem.*, 222 (1994) 183–194.
- [31] M. Dubois, K.A. Gilles, J.K. Hamilton, P.A. Rebers, and F. Smith, *Anal. Chem.*, 28 (1956) 350–356.
- [32] O. Holst, L. Brade, P. Kosma, and H. Brade, *J. Bacteriol.*, 173 (1991) 1862–1866.
- [33] U.K. Laemmli and M. Favre, *J. Mol. Biol.*, 80 (1973) 575–599.
- [34] T. Komuro and C. Galanos, *J. Chromatogr.*, 450 (1988) 381–387.
- [35] C.-M. Tsai and C.E. Frasch, *Anal. Biochem.*, 119 (1982) 115–119.
- [36] H. Masoud, E. Altman, J.C. Richards, and J.S. Lam, *Biochem.*, 33 (1994) 10568–10578.
- [37] W.S. York, A.G. Darvill, M. McNeil, T.T. Stevenson, and P. Albersheim, *Methods Enzymol.*, 118 (1985) 3–40.
- [38] I. Sadovskaya, J.-R. Brisson, E. Altman, and L.M. Mutharia, *Carbohydr. Res.*, 283 (1996) 111–127.
- [39] H.I. Hakomori, *J. Biochem.*, 66 (1964) 205–208.
- [40] A.J. Mort, S. Parker, and M.-S. Kuo, *Anal. Biochem.*, 133 (1983) 380–384.
- [41] K.P. Bateman, R.L. White, and P. Thibault, *Rapid Commun. Mass Spectrom.*, 11 (1997) 307–315.
- [42] D. Uhrin, J.R. Brisson, G. Kogan, and H.J. Jennings, *J. Magn. Reson.*, B104 (1994) 289–293.